Identification of Frequency-dependent Viscous Damping

Andrew Ross
Centre for Ships and Ocean Structures (CeSOS)
Norwegian University of Science and Technology (NTNU)
NO-7491 Trondheim, Norway
Email: andrew.ross@marin.ntnu.no

Thor I. Fossen
Department for Engineering Cybernetics (ITK)
Norwegian University of Science and Technology (NTNU)
NO-7491 Trondheim, Norway
Email: fossen@ieee.org

***Abstract*— This paper analyses the nature of the linear viscous damping terms present in a ship model. An analytical solution for a transfer function model of these terms is presented, and a simplification introduced such that these terms can be identified in the time domain for use in simulation and modelling.**

I. Introduction

In recent years, much effort has been spent in developing a unified mathematical model to describe the motion of a ship. Historically two decoupled models were used: a *manoeuvring* model and a *seakeeping* model. These were developed separately and out of different motivations. A manoeuvring model describes the motion of a ship in calm water, while a seakeeping model describes the response of the ship in the presence of waves. For a comprehensive treatise on manoeuvring models, see the work by Clarke in [1]. For the development of seakeeping models see [2] or [3]. The unification of the two was described by Bailey et. al. in [4] and has been further developed by Fossen in [5], using the results of Kristiansen [6]. The unification of the two allows for a very concise, accurate and comprehensive simulation model. With the use of strip theory, a fairly complete simulation model is made available quickly and easily. The major deficiency here is that potential theory does not describe low frequency damping. This is perfectly sensible, since at these frequencies, skin friction and other viscous terms dominate. Simply adding the conventional manoeuvring hydrodynamic derivatives to the model is unsatisfactory, since these are known to die off quickly with frequency. A route typically taken is to add a damping term which decays exponentially with frequency, and enters the system linearly with velocity. This is an ad-hoc method, and comes from practical rather than theoretical motivation. It does, however, match up very well with experimental results. This model augmentation can be interpreted as a generalisation of the hydrodynamic derivatives. At steady speed in calm water, the model matches the conventional low speed manoeuvring model, but more accurately predicts behaviour in the crossover region between the manoeuvring model and seakeeping model. This paper contributes by showing how this frequency dependent model can be identified from time domain experimentation.The resulting model is accurate, and yet is still very suitable for simulation and control purposes.

A. Notation

Vectors are in lower case bold text, and matrices are in upper-case bold. The convolution of two functions is denoted by

$$(a * b)(t) = \int_0^t a(t-\tau)\, b(\tau)\, d\tau$$

Given two vectors $\mathbf{a} \in \mathbb{R}^n$ and $\mathbf{b} \in \mathbb{R}^n$, the convolution is given in an implicit form such that each individual convolution is summed

$$\begin{aligned} (\mathbf{a} * \mathbf{b})(t) &= \sum_{i=1}^{n} (a_i * b_i)(t) \\ &= \sum_{i=1}^{n} \int_0^t a_i(t-\tau)\, b_i(\tau)\, d\tau \\ &= (a_1 * b_1)(t) + ... + (a_n * b_n)(t) \end{aligned}$$

The convolution of a matrix with a vector implies that each row of the matrix is taken to be a vector, and convolved as above, the output being a vector of convolutions.

B. Hydrodynamic Model

The classical hydrodynamic model is written as follows

$$\begin{aligned} (\mathbf{M}_{RB} + \mathbf{A}(\omega))\, \ddot{\boldsymbol{\eta}} + \mathbf{B}(\omega)\, \dot{\boldsymbol{\eta}} & \\ + \mathbf{g}(\boldsymbol{\eta}) &= \boldsymbol{\tau} + \boldsymbol{\tau}_{FK+D} \end{aligned} \quad (1)$$

where $\boldsymbol{\eta} \in \mathbb{R}^3 \times S^3$ is the generalised position in the North East Down (NED) frame, $\mathbf{M}_{RB} \in \mathbb{R}^{6\times6}$ is the rigid body mass, $\mathbf{A}(\omega) \in \mathbb{R}^{6\times6}$ is the added mass, $\mathbf{B}(\omega) \in \mathbb{R}^{6\times6}$ is the linear damping matrix and includes both potential and viscous damping such that $\mathbf{B}(\omega) = \mathbf{B}_p(\omega) + \mathbf{B}_v(\omega)$, where the subscripts p and v mean potential and viscous damping respectively. An example of the $B_{22}(\omega)$ function is plotted in Figure 1, using a generic form for $B_{v22}(\omega)$. $\mathbf{g}(\boldsymbol{\eta}) \in \mathbb{R}^6$ is the vector of restoring forces, $\boldsymbol{\tau} \in \mathbb{R}^6$ is the vector of control force inputs and, finally, $\boldsymbol{\tau}_{FK+D} \in \mathbb{R}^6$ is the vector of Froude-Krylov and diffraction forces.

From Cummins and Ogilvie in [7] and [8] we know that the time-domain solution for this frequency dependent model can be written as

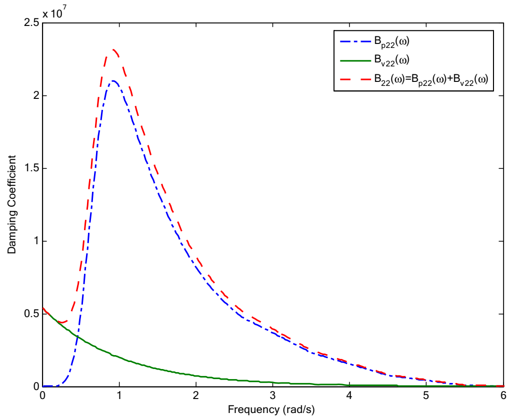

Fig. 1. Example of $B_{22}(\omega)$: a linear damping coefficient

$$\begin{aligned}(\mathbf{M}_{RB}+\mathbf{A}(\infty))\ddot{\boldsymbol{\eta}}+\mathbf{B}(\infty)\dot{\eta}&\\ +(\mathbf{K}*\dot{\boldsymbol{\eta}})(t)+\mathbf{g}(\eta) &= \boldsymbol{\tau}+\boldsymbol{\tau}_{FK+D} \qquad (2)\end{aligned}$$

where $\mathbf{K} \in \mathbb{R}^{6\times 6}$ is a matrix of impulse response functions where each component is formed according to

$$k_{ij}(t)=\frac{2}{\pi}\int_0^{\infty}(B_{ij}(\omega)-B_{ij}(\infty))\cos(\omega t)\,d\omega \quad i,j=1,..,6$$

A recent development of this is a more concise form where the potential damping forces in $\mathbf{B}(\omega)$ are described by low-order state space models. The ship model used throughout this paper is from [5] and takes the following form:

$$\dot{\boldsymbol{\eta}} = \mathbf{J}(\boldsymbol{\theta})\boldsymbol{\nu} \qquad (3)$$

$$\mathbf{M}\dot{\boldsymbol{\nu}}+\mathbf{d}_l(\boldsymbol{\nu})+\boldsymbol{\mu}_p+\mathbf{g}(\boldsymbol{\eta}) = \boldsymbol{\tau}+\boldsymbol{\tau}_{FK+D} \qquad (4)$$

$$\dot{\boldsymbol{\chi}} = \mathbf{A}_r\boldsymbol{\chi}+\mathbf{B}_r\boldsymbol{\nu} \qquad (5)$$

$$\boldsymbol{\mu}_p = \mathbf{C}_r\boldsymbol{\chi}+\mathbf{D}_r\boldsymbol{\nu} \qquad (6)$$

where $\boldsymbol{\nu} \in \mathbb{R}^6$ is the velocity in the body-fixed frame, $\mathbf{J}(\boldsymbol{\theta}) \in \mathbb{R}^{6\times 6}$ is a rotation matrix from the body-fixed frame to the NED frame (with $\boldsymbol{\theta}=\boldsymbol{\eta}_{4,5,6}$), $\mathbf{M} \in \mathbb{R}^{6\times 6} = \mathbf{M}_{RB} + \mathbf{M}_A(\infty)$ is the rigid body mass plus the added mass at infinite frequency, $\mathbf{d}_l(\boldsymbol{\nu}) \in \mathbb{R}^6$ is the vector of all linear damping forces except for those described by potential theory and $\boldsymbol{\mu}_p \in \mathbb{R}^6$ is the vector of potential damping forces. These are modelled using a state space formulation from [6] where the state space model in equations (5)-(6) gives these frequency varying forces.

Remark 1: The models present here apply for station-keeping and low-speed manoeuvring, but not for high speed manoeuvres, since they do not account for the coriolis-centripetal terms, or nonlinear damping.

C. Problem Description

With the system given by equations (3)-(6), the modelling problem is almost complete. Almost all the terms in these equations can be found. The form of $\mathbf{B}_p(\omega)$ is easily available from potential-theory based programs, and so the state-space model for the time domain solution, $\boldsymbol{\mu}_p$, of these forces is readily available. Unfortunately, far less is known about $\mathbf{B}_v(\omega)$ than about $\mathbf{B}_p(\omega)$, and so a time-domain solution is elusive at present, i.e. $\mathbf{d}_l(\boldsymbol{\nu})$ is basically unknown. Essentially, $\mathbf{d}_l(\boldsymbol{\nu})$ describes those forces which are awkward and time-consuming to derive theoretically, and difficult to find experimentally. The contribution of this paper is to attempt to account for these. In typical control plant models of a ship, this $\mathbf{d}_l(\boldsymbol{\nu})$ would be the linear hydrodynamic damping derivatives, i.e. $\mathbf{B}(0)$. This approach is weak, since it assumes that the damping forces are invariant with respect to frequency, which is known to be incorrect. This paper proposes a more complete description of these forces.

II. Form of $\mathbf{d}_l(\nu)$

If the impulse response of these damping forces is known, then the precise time domain solution for $\mathbf{d}_l(\boldsymbol{\nu})$ can be written as the impulse response convolved with $\boldsymbol{\nu}$ as follows:

$$\mathbf{d}_l(\boldsymbol{\nu}) = (\mathbf{K}*\boldsymbol{\nu})(t) \qquad (7)$$

$$\mathbf{d}_l(\boldsymbol{\nu}) = \int_0^t \mathbf{K}(t-\tau)\boldsymbol{\nu}(\tau)\,\mathbf{d}\boldsymbol{\tau} \qquad (8)$$

where $\mathbf{K}(t) \in \mathbb{R}^{6\times 6}$ is a matrix of impulse response functions, i.e. $\mathbf{K}(t)=\{k_{ij}\}$, $i,j=1,..6$. To stop and take stock of where this has led, excuse the following abuse of notation to describe the system:

$$d_{li} = (\mathbf{k}_i*\boldsymbol{\nu})(t)=\sum_{j=1}^{6}(k_{ij}*\nu_j)(t) \qquad (9)$$

$$\mathbf{k}_i = \begin{bmatrix}k_{i1} & k_{i2} & k_{i3} & k_{i4} & k_{i5} & k_{i6}\end{bmatrix}$$

with each $\mathbf{k}_i(t) \in \mathbb{R}^6$ $(i=1,..,6)$ being a row-vector of impulse response functions, where i denotes the degree of freedom. In words, each degree of freedom has six convolution functions: one for each of the body-fixed velocities, giving 36 convolution terms in total. Although more complicated than is preferable, it leads to a more precise description of the damping forces. Consider if the convolution were irrelevant, and that the linear viscous damping could be completely described by the matrix of hydrodynamic derivatives $\mathbf{D}=\{d_{ij}\}$, $i,j=1,..,6$:

$$\mathbf{d}_l(\boldsymbol{\nu}) = \mathbf{D}\boldsymbol{\nu}$$

$$d_{li}(\boldsymbol{\nu}) = \sum_{j=1}^{6} d_{ij}\nu_j \qquad (10)$$

Noting the similarities between equations (9) and (10), what we have is nothing more than a generalisation of the typical hydrodynamic derivatives to include the memory effects present in the fluid. This is a more precise and rigorous description of the physical effects of damping, although an additional layer of complication is added. Therefore as a first step, an analytical solution for the impulse response functions in (8) should be found.

III. Low Frequency Time Domain Simulation

Analysing the low-frequency response of a ship is vital for any kind of manoeuvring problem. Since several terms in the hydrodynamic model vary with frequency, the general assumption is that it is possible to simply select the values of these terms at zero frequency, such that the equations take the form

$$(\mathbf{M}_{RB} + \mathbf{M}_A(0))\,\dot{\boldsymbol{\nu}} + \mathbf{D}\boldsymbol{\nu} + \mathbf{g}(\boldsymbol{\eta}) = \tau \qquad (11)$$

where

$$\mathbf{D} = -\begin{bmatrix} X_u & X_v & X_w & X_p & X_q & X_r \\ Y_u & Y_v & Y_w & Y_p & Y_q & Y_r \\ Z_u & Z_v & Z_w & Z_p & Z_q & Z_r \\ K_u & K_v & K_w & K_p & K_q & K_r \\ M_u & M_v & M_w & M_p & M_q & M_r \\ N_u & N_v & N_w & N_p & N_q & N_r \end{bmatrix}$$

$$\mathbf{M}_A(0) = -\begin{bmatrix} X_{\dot u} & X_{\dot v} & X_{\dot w} & X_{\dot p} & X_{\dot q} & X_{\dot r} \\ Y_{\dot u} & Y_{\dot v} & Y_{\dot w} & Y_{\dot p} & Y_{\dot q} & Y_{\dot r} \\ Z_{\dot u} & Z_{\dot v} & Z_{\dot w} & Z_{\dot p} & Z_{\dot q} & Z_{\dot r} \\ K_{\dot u} & K_{\dot v} & K_{\dot w} & K_{\dot p} & K_{\dot q} & K_{\dot r} \\ M_{\dot u} & M_{\dot v} & M_{\dot w} & M_{\dot p} & M_{\dot q} & M_{\dot r} \\ N_{\dot u} & N_{\dot v} & N_{\dot w} & N_{\dot p} & N_{\dot q} & N_{\dot r} \end{bmatrix}$$

This solution simply uses the hydrodynamic derivatives, which are coefficients corresponding to the zero frequency values of the generalised damping and added-mass forces, and so equation (11) is used in a conventional state space model of a ship. There is an error in this methodology: the assumption of a zero-frequency added mass term is in fact incorrect. In [7] and [8] it was shown how to convert the frequency model into its equivalent time-domain solution. By adapting their notation to match ours, the time-domain solution is as follows:

$$\begin{aligned}(\mathbf{M} + \mathbf{M}_A(\infty))\,\dot{\boldsymbol{\nu}} + \boldsymbol{\mu}_p + \mathbf{d}_l(\boldsymbol{\nu}) & \\ + \mathbf{g}(\boldsymbol{\eta}) &= \boldsymbol{\tau} + \boldsymbol{\tau}_{FK+D} \qquad (12)\end{aligned}$$

where $\mathbf{d}_l(\boldsymbol{\nu})$ comes from the convolution integrals in equation (8). So an example of this in the x-axis alone, neglecting the potential damping, which is dominated by viscous at LF, would be

$$\begin{aligned}(m + a_{11}(\infty))\,\dot{u} + (k_{11} * u)(t) &= \tau_{1,env} + \tau_1 \qquad (13)\\ \dot{x} &= u \qquad (14)\end{aligned}$$

where $\tau_{1,env}$ can consist of any environmental loads, such as the Froude-Krylov, current, and wind forces. Now that it has been made clear how the correct time-domain formulation should be constructed, the problem of obtaining these impulse response functions must now be tackled.

IV. Impulse Response Functions

This section is primarily functional analysis, and the vectorised notation is set aside for the moment. The form of the impulse response function is wholly dependent on the frequency response of the damping function, denoted by $B_v(\omega)$. This being the case, the impulse response function can be found as follows:

$$K(t) = \frac{2}{\pi}\int_0^\infty (B_v(\omega) - B_v(\infty))\cos(\omega t)\,d\omega \qquad (15)$$

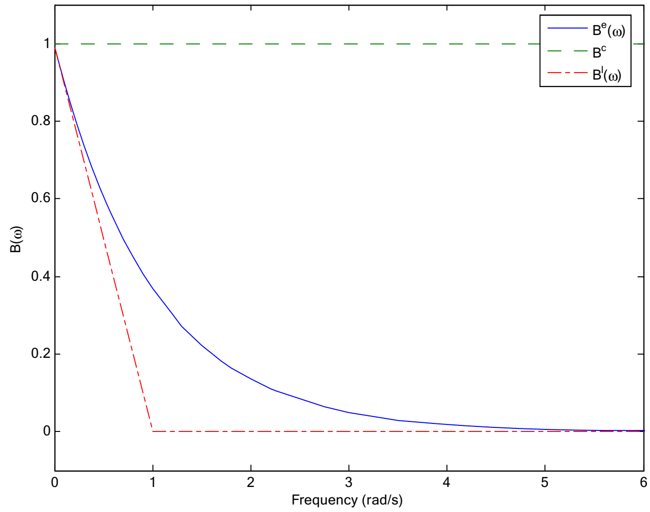

Fig. 2. Three $B(\omega)$ candidates

There are several candidates for what form $B(\omega)$ should take. The three most common are:

1) $B^e(\omega) = \beta\exp(-\alpha\omega)$
2) $B^l(\omega) = \beta\left(1 - \frac{\omega}{\alpha}\right), \omega \le a,\ B^l(\omega) = 0$ for $\omega > \alpha$
3) $B^c = \beta$

The third one is recognisable as the conventional hydrodynamic derivative. The second is a linear ramp function, and the first is an exponential ramp function, proposed by Bailey et. al. in [4]. It is this first one that is analysed within this paper, as it possesses convenient properties and is generally very well behaved. Generic examples of these three functions are shown in Figure 2, with $\beta, \alpha = 1$.

A. Convolution Example

Here we analyse the damping force in surge from equation (13) for a constant velocity (a step input at $t = 0$). Taking the exponential ramp function, setting $\beta = X_u$, and implementing the integral in (15), which is now a damped exponential cosine integral, seen for example at [9], then the following is derived

$$\begin{aligned}k_{11}(t) &= \frac{2}{\pi}\int_0^\infty X_u\exp(-\alpha\omega)\cos(\omega t)\,d\omega \qquad (16)\\ k_{11}(t) &= 2\frac{X_u}{\pi}\frac{\alpha}{\alpha^2 + t^2} \qquad (17)\end{aligned}$$

which then gives us the time domain solution for a constant velocity as

$$\begin{aligned} d_1(\nu) &= \int_0^t k_{11}(t-\tau)\,u(\tau)\,d\tau && (18)\\ &= u\frac{2\alpha X_u}{\pi}\int_0^t \frac{d\tau}{a^2+(t-\tau)^2} \\ d_1(\nu) &= \frac{2X_u}{\pi}\arctan\left(\frac{t}{\alpha}\right)u && (19)\\ \lim_{t\to\infty} d_1(v) &= X_u u && (20)\end{aligned}$$

This means that at a steady speed, the damping force in surge can be properly described by a constant coefficient, which can easily be seen to correspond to the conventional hydrodynamic derivative. This is perfectly sensible, since a steady speed in some sense corresponds to a zero-frequency input, and so in this case the function should be equal to the conventional model. Implementing the convolution integration for anything other than very simple forms of u is extremely difficult. Therefore, although this formulation is accurate, it is hardly convenient either for simulation or control system design. To facilitate these tasks, we instead take an approach using Laplace transforms, with the goal of deriving transfer functions and hence giving a nice, comprehensible and convenient formulation of the above equations.

V. Laplace Derivations

The use of Laplace transforms on (7) and (8) is very useful, as this framework is perfect for simplifying the annoyingly complicated convolution terms. Furthermore, any result will fit in extremely nicely with control system design, the output being composed of transfer functions. Recall that to get the damping forces, we convolve the impulse response functions with the body-fixed velocities, and note that the Laplace transform of a convolution is the Laplace transform of the first function, multiplied by the transform of the function that it is convolved with such that we have:

$$\begin{aligned} d_l(\nu) &= (K*\nu)(t) \\ \mathcal{L}[d_l(\nu)] &= \mathcal{L}[K(t)]\times\mathcal{L}[\nu(t)] \\ d_l(s) &= H(s)\,\nu(s)\end{aligned}$$

where $H(s)=\mathcal{L}[K(t)]$. From this it is easily seen that the equations are now formed such that we have $H(s)$: a transfer function. This is highly convenient for implementation purposes, and so now the problem moves on to finding what form the transfer function takes given the form of $K(t)$ from equation (17). Recall that the Laplace transform for a function is given by

$$F(s)=\mathcal{L}[f(t)]=\int_0^\infty \exp(-st)\,f(t)\,dt$$

so to find the Laplace transform we perform the following

$$\begin{aligned} H(s) &= \int_0^\infty \exp(-st)\,K(t)\,dt && (21)\\ &= \int_0^\infty \exp(-st)\left[\frac{2}{\pi}\int_0^\infty B(\omega)\cos(\omega t)\,d\omega\right]dt \\ &= \frac{2}{\pi}\int_0^\infty B(\omega)\left[\int_0^\infty \exp(-st)\cos(\omega t)\,dt\right]d\omega \\ H(s) &= \frac{2}{\pi}\int_0^\infty B(\omega)\frac{s}{s^2+\omega^2}d\omega && (22)\end{aligned}$$

where this equation holds for an arbitrary $B(\omega)$. We use $B(\omega)=\beta\exp(-\alpha\omega)$ and derive the following

$$\begin{aligned} H(s) &= \frac{2\beta}{\pi}\int_0^\infty \exp(-\alpha\omega)\frac{s}{s^2+\omega^2}d\omega && (23)\\ H(s) &= \frac{\beta}{\pi}2ci(\alpha s)\sin(as)+ \\ &\quad (\pi-2si(\alpha s)\cos(\alpha s)) && (24)\end{aligned}$$

where $ci(\cdot)$ and $\sin(\cdot)$ are given in the appendix. We can then write out a transfer function such that

$$H(s)=|H(s)|\,\angle H(s)$$

where

$$\begin{aligned} |H(s)| &= \sqrt{\mathrm{Re}[H(s)]^2+\mathrm{Im}[H(s)]^2} \\ \angle H(s) &= \arctan\frac{\mathrm{Im}[H(s)]}{\mathrm{Re}[H(s)]}\end{aligned}$$

The real and imaginary components of the individual parts of equation (24) are given in the appendix, and using these, we derive the following solution

$$\begin{aligned} |H(s)| &= \beta(\exp(-2\alpha\omega)+\frac{4}{\pi^2}(Chi(\alpha\omega)\sinh(\alpha\omega) \\ &\quad -Shi(\alpha\omega)\cosh(\alpha\omega))^2)^{0.5} && (25)\\ \angle H(s) &= \arctan\frac{2}{\pi}(\exp(\alpha\omega)(Chi(\alpha\omega)\sinh(\alpha\omega) \\ &\quad -\cosh(\alpha\omega)Shi(\alpha\omega))) && (26)\end{aligned}$$

$Shi(\cdot)$ and $Chi(\cdot)$ are defined in the appendix. This transfer function is clearly very complicated, but in form it resembles a low-pass filter. The transfer function has the following notable limits

$$\begin{aligned} \lim_{s\to 0}|H(s)| &= \beta \\ \lim_{s\to\infty}|H(s)| &= 0 \\ \lim_{s\to 0}\angle H(s) &= 0 \\ \lim_{s\to\infty}\angle H(s) &= -\frac{\pi}{2}\end{aligned}$$

A. Filter Approximation

Instead of a direct identification of $H(s)$, we instead identify a state space approximation of the transfer function, $H_a(s)$ corresponding to a stable filter:

$$H_a(s) = \frac{b_0}{a_1 s + a_0} \tag{27}$$

This approximation is fairly close to the analytical solution shown in equation (25) and (26). So we form a standard parameterisation from [10] such that we have:

$$\begin{aligned} y &= d_l(\nu) \\ \dot{\boldsymbol{\phi}}_1 &= \boldsymbol{\lambda}_c \boldsymbol{\phi}_1 + \mathbf{l}u \\ \dot{\boldsymbol{\phi}}_2 &= \boldsymbol{\lambda}_c \boldsymbol{\phi}_2 - \mathbf{l}y \\ y &= \boldsymbol{\theta}_{\lambda}^{*\top} \boldsymbol{\phi} \\ z &= \boldsymbol{\theta}^{*\top} \boldsymbol{\phi} \end{aligned}$$

where

$$\begin{aligned} \boldsymbol{\phi} &= \begin{bmatrix} \boldsymbol{\phi}_1^\top & \boldsymbol{\phi}_2^\top \end{bmatrix}^\top \\ \theta_{\lambda}^* &= \begin{bmatrix} b_0 & a_1 & a_0 \end{bmatrix}^\top \\ \theta_c^* &= \begin{bmatrix} b_0 & a_1 - \lambda_1 & a_0 - \lambda_0 \end{bmatrix} \\ \boldsymbol{\lambda}_c &= \begin{bmatrix} -\lambda_1 & -\lambda_0 \\ 1 & 0 \end{bmatrix} \end{aligned}$$

where λ_c is a standard stable filter. Many update laws may be used. The following update law is just one example:

$$\begin{aligned} \dot{\hat{\boldsymbol{\theta}}} &= \boldsymbol{\Gamma} \varepsilon \boldsymbol{\phi}, \quad \boldsymbol{\Gamma} > \mathbf{0} \\ \varepsilon &= z - \hat{z} \\ \boldsymbol{\phi} &= [\boldsymbol{\phi}_1, \boldsymbol{\phi}_2]^\top \end{aligned} \tag{28}$$

For convergence properties of this algorithm, see [10]. The bode plot of the approximation against the analytical solution is shown here in Figure 3. This is for $\beta = 2000$, $\alpha = 1$. At higher frequencies, the difference in magnitude between the two grows, but the gain at these frequencies is small. The phase response is similar across all frequencies.

Remark 2: Substituting a filter into the problem here is extremely similar to the conventional situation of filtering away the wave frequencies, but the theoretical justification is present here

VI. Final Form

So the system that we are identifying looks as follows

$$\begin{aligned} \dot{\boldsymbol{\eta}} &= \mathbf{J}(\boldsymbol{\theta}) \boldsymbol{\nu} & (29) \\ \mathbf{M}\dot{\boldsymbol{\nu}} + \boldsymbol{\mu}_v + \boldsymbol{\mu}_p + \mathbf{g}(\boldsymbol{\eta}) &= \boldsymbol{\tau} + \boldsymbol{\tau}_{FK+D} & (30) \\ \dot{\boldsymbol{\chi}} &= \mathbf{A}_r \boldsymbol{\chi} + \mathbf{B}_r \boldsymbol{\nu} & (31) \\ \boldsymbol{\mu}_p &= \mathbf{C}_r \boldsymbol{\chi} + \mathbf{D}_r \boldsymbol{\nu} & (32) \\ \boldsymbol{\mu}_v &= \mathbf{H}_v(s) \boldsymbol{\nu}(s) & (33) \end{aligned}$$

where $\boldsymbol{\mu}_v$ is the vector of viscous damping forces, and $\mathbf{H}_v(s)$ is a 6×6 matrix of transfer functions. Each transfer function can be either the analytical solution from (25) and (26), or the approximation from equation (27). Although there are 36 possible transfer functions, in practice, much of the cross coupling equations are known to be zero across the spectrum. The other terms are the same as before.

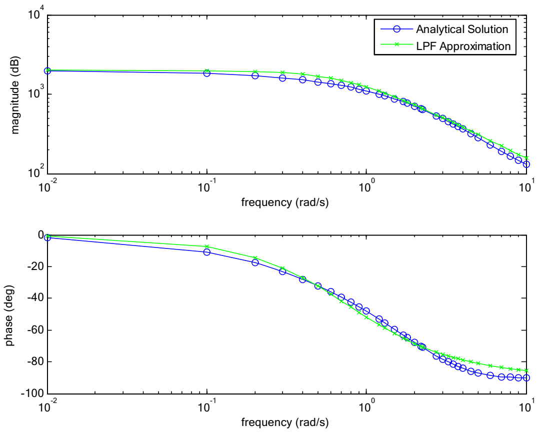

Fig. 3. Bode plot of $H(s)$ and $H_a(s)$

VII. Conclusions

This paper has shown a new framework by which the damping forces acting on a ship can be better modelled and understood. Although the transfer function developed turned out to be extremely complex, and not well-suited for identification, the approximation was shown to be very close, and useful for identification or adaptive control. The system described by equations (29)-(33) is very well suited for modelling and control purposes, and accounts for most effects present in low-speed manoeuvring or seakeeping, while retaining almost all of the accuracy of the analytical model.

Future work will focus on augmenting this model with coriolis-centripetal effects and nonlinear damping terms.

VIII. Acknowledgment

This work was funded by the Research Council of Norway through the Centre for Ships and Ocean Structures (CeSOS).

Appendix

$si(\cdot)$ and $ci(\cdot)$ denote the sinintegral and cosineintegral functions:

$$ci(x) = \int_x^\infty \frac{\cos t}{t} dt \tag{34}$$

$$si(x) = \int_x^\infty \frac{\sin t}{t} dt \tag{35}$$

The following identities are used to derive (25) and (26)

$$
\begin{aligned}
\operatorname{Re} ci\left(\alpha j\omega\right) &= Chi\left(\alpha\omega\right) \\
\operatorname{Im} ci\left(\alpha j\omega\right) &= \frac{\pi}{2} \\
\operatorname{Re}\sin\left(\alpha j\omega\right) &= 0 \\
\operatorname{Im}\sin\left(\alpha j\omega\right) &= \sinh\left(\alpha\omega\right) \\
\operatorname{Re}\left[ci\left(\alpha jw\right)\sin\left(\alpha jw\right)\right] &= -\frac{\pi}{2}\sinh\left(\alpha\omega\right) \\
\operatorname{Im}\left[ci\left(\alpha jw\right)\sin\left(\alpha jw\right)\right] &= \sinh\left(\alpha jw\right) Chi\left(\alpha w\right) \\
\operatorname{Re}\left[si\left(\alpha jw\right)\cos\left(\alpha jw\right)\right] &= 0 \\
\operatorname{Im}\left[si\left(\alpha jw\right)\cos\left(\alpha jw\right)\right] &= Shi\left(\alpha\omega\right)\cosh\left(\alpha\omega\right) \\
\operatorname{Re}\left[\pi\cos\left(\alpha jw\right)\right] &= \pi\cosh\left(\alpha\omega\right) \\
\operatorname{Im}\left[\pi\cos\left(\alpha jw\right)\right] &= 0
\end{aligned}
$$

where

$$
\begin{aligned}
Chi\left(x\right) &= \gamma + \ln x + \int_0^x \frac{\cosh t - 1}{t} dt \\
Shi\left(x\right) &= \int_0^x \frac{\sinh t}{t} dt
\end{aligned}
$$

where γ is the Euler-Mascheroni constant. We can then move on and define the real and imaginary components as:

$$
\begin{aligned}
\operatorname{Re}\left[H\left(s\right)\right] &= \frac{\beta}{\pi}(2\operatorname{Re}\left[ci\left(\alpha jw\right)\sin\left(\alpha jw\right)\right] + \qquad (36) \\
&\quad \operatorname{Re}\left[\left(\pi - 2si\left(\alpha jw\right)\right)\cos\left(\alpha jw\right)\right]) \\
&= \frac{\beta}{\pi}\left(2\times -\frac{\pi}{2}\sinh\left(\alpha\omega\right) + \pi\cosh\left(\alpha\omega\right)\right) \\
&= \beta\left(\cosh\left(\alpha\omega\right) - \sinh\left(\alpha\omega\right)\right) \\
\operatorname{Re}\left[H\left(s\right)\right] &= \beta\exp\left(-\alpha\omega\right) \qquad (37)
\end{aligned}
$$

$$
\begin{aligned}
\operatorname{Im}\left[H\left(s\right)\right] &= \frac{\beta}{\pi}(2\operatorname{Im}\left[ci\left(\alpha jw\right)\sin\left(\alpha jw\right)\right] + \qquad (38) \\
&\quad \operatorname{Im}\left[\left(\pi - 2si\left(\alpha jw\right)\right)\cos\left(\alpha jw\right)\right]) \\
&= \frac{2\beta}{\pi}(\sinh\left(\alpha\omega\right) Chi\left(\alpha\omega\right) - \\
&\quad \cosh\left(\alpha\omega\right) Shi\left(\alpha\omega\right)) \qquad (39)
\end{aligned}
$$

And from here we can calculate (25) and (26).

REFERENCES

[1] D. Clarke, "The foundations of steering and maneuvering," in *Proceedings of the IFAC Conference on Control Applications*, 2003, Plenary talk.

[2] O. M. Faltinsen, *Sea Loads on Ships and Offshore Structures*. Cambridge University Press, 1990.

[3] J. Journée and W. Massie, *Offshore Hydromechanics*. The Netherlands: Delft University of Technology, 2001.

[4] P. Bailey, W. Price, and P. Temarel, "A unified mathematical model describing the manoeuvring of a ship travelling in a seaway," *Transactions of the Royal Institute of Naval Architects*, vol. 140, pp. 131–149, 1998.

[5] T. Fossen, "A nonlinear unified state space model for ship maneuvering and control in a seaway," *Journal of Bifurcation and Chaos*, 2005.

[6] E. Kristiansen, "State space representation of hydrodynamic memory effects," Ph.D. dissertation, Norwegian University of Science and Technology, 2005.

[7] W. Cummins, "The impulse response function and ship motions," David Taylor Model Basin, Hydromechanics Laboratory, USA, Tech. Rep. 1661, 1962.

[8] T. Ogilvie, "Recent progress towards the understanding and prediction of ship motions," in *Symposium on Naval Hydrodynamics*, 1964, pp. 3–79.

[9] E. Weinstein, "Damped exponential cosine integral," *Mathword- A Wolfram Resource*, p. mathworld.wolfram.com/DampedExponentialCosineIntegral.html, 2005.

[10] P. Ioannou and J. Sun, *Robust Adaptive Control*. Trondheim: Tapir Akademisk Forlag, 2003.